

Smoluchowski equations for linker-mediated irreversible aggregation

J. M. Tavares,^{1,2,*} G. C. Antunes,^{3,1,4,5,†} C. S. Dias,^{3,1,‡} M. M. Telo da Gama,^{3,1,§} and N. A. M. Araújo^{3,1,¶}

¹*Centro de Física Teórica e Computacional, Universidade de Lisboa, 1749-016 Lisboa, Portugal*

²*Instituto Superior de Engenharia de Lisboa, ISEL,*

Avenida Conselheiro Emídio Navarro, 1 1950-062 Lisboa, Portugal

³*Departamento de Física, Faculdade de Ciências,*

Universidade de Lisboa, 1749-016 Lisboa, Portugal

⁴*Max Planck Institute for Intelligent Systems, Stuttgart, Germany*

⁵*Institute for Theoretical Physics IV, University of Stuttgart, Pfaffenwaldring 57, 70569 Stuttgart, Germany*

In order to study linker-mediated aggregation of colloidal particles with limited valence, we combine kinetic Monte Carlo simulations and an approximate theory based on the Smoluchowski equations. We found that aggregation depends strongly on two parameters, the ratio of the number of linkers and particles and the ratio of their diffusion coefficients. These control parameters are absent in single-species aggregation and provide a much greater variety and control of the resulting structures. We show that aggregation is non-trivial when two time scales of aggregation are present. Our aggregation dynamics theory is in qualitative and quantitative agreement with kinetic Monte Carlo simulations. Our results show how the optimal aggregation may be tuned through the ratio of the linkers and particles and that of the diffusion coefficients.

I. INTRODUCTION

The self-assembly of micron-sized building blocks poses various challenges from the practical and theoretical points of view, since the interaction between the particles is of the order of the thermal fluctuations [1–12]. Recently, the aggregation mediated by linkers has been attracting increasing attention [12–15]. The addition of a second species to the aggregation process increases the range of the assembled structures and adds another layer of control. Different aggregation regimes [16] or unexpected mechanical properties [17] may be obtained just by tuning the concentration of the linkers.

Theoretically, the focus has been on equilibrium properties [18–20], where richer phase diagrams have been reported. Some work addressed the dynamics, although most theoretical studies considered the limit where the particles and linkers diffuse much faster than the aggregates [13], or the early stages of aggregation [21]. Here, we present a generalized theory, where we consider the dependence of the dynamics on three relevant factors: (i) the difference in the diffusion coefficients of the particles and linkers (i.e. the existence of at least two time scales); (ii) the concentration or the relative number of particles and linkers and (iii) the restrictions on the aggregation imposed by the maximum number of bonds per particle. As effects such as the density dependence of the diffusion coefficients, aggregation reaction times, correlations between bonds, or spatial and topological properties of the clusters, have been extensively studied for aggregation without linkers, we will neglect or oversimplify them.

To study the dynamics of aggregation, we apply a framework based on a generalized Smoluchowski equation. This formulation has been widely used, ranging from studies of the rings of Saturn, to interstellar dust grains, to disinfection with bacteriophages, or even the aggregation of proteins in milk [22–25]. We solve the Smoluchowski equations and compare the results to particle-based simulations using kinetic Monte Carlo, where we neglect the shape of the clusters and focus on their spatial distribution.

The paper is organized as follows. In Sec. II, we introduce the model for linker-mediated aggregation, the numerical simulations of the model, the corresponding Smoluchowski equations, and the approximate analytical theory. In Sec. III, we present the results for the asymptotic limit, and the time evolution of both the bonding fraction and the size distribution of the clusters, obtained from the simulations and via the approximate theory. We discuss our results and draw some conclusions in Sec. IV.

II. MODEL

A. Model description

We consider a mixture of N_P particles and of N_L linkers. Particles and linkers diffuse and bond irreversibly upon encounter. The linkers mediate the bonding of the particles: two particles become bonded when one of them bonds to a linker that is already bonded to another particle. Two bonded particles belong to the same cluster (and this defines a cluster as the set of particles that belong to it). Each linker bonds to a maximum of two particles and each particle bonds to a maximum of f linkers. As a consequence, each linker can be in one of three states: not bonded to any particle (state 0, free linker), bonded to one particle only (state 1) or bonded to two particles (state 2). N_i is the number of linkers in state

* jmtavares@fc.ul.pt

† antunes@is.mpg.de

‡ csdias@fc.ul.pt

§ mmgama@fc.ul.pt

¶ nmaraujo@fc.ul.pt

i (so that $N_0 + N_1 + N_2 = N_L$). In this model the linkers control the extent of aggregation of the particles, and to quantify this effect we use the parameter ϕ , the ratio between the actual number of linkers and the maximum number of linkers that could be bonded to all particles,

$$\phi = \frac{N_L}{fN_P}. \quad (1)$$

In what follows we focus on the dependence on three factors: (i) the difference in the diffusion coefficients of particles and linkers; (ii) the relative number of particles and linkers (i.e. the role of ϕ in the dynamics) and (iii) the particle valence f .

The size i of a cluster is the number of particles that belong to it. We assume that two particles that are bonded to each other are connected by only one linker (no double bonding) and that the clusters are tree like (no loops). Therefore, a cluster of size i contains $i-1$ linkers in state 2, corresponding to the number of bonds needed to form it. Each cluster of size i contains also a number j of linkers in state 1 in the interval $[0; w_i]$, with $w_i = (f-2)i+2$. Notice that a particle with no linkers bonded to it is a cluster of size $i=1$ with $j=0$. It is useful to consider that a cluster of size i has a total of w_i bonding sites on its “surface”; if it contains j linkers in state 1, then j of these sites are occupied (by a linker) and $w_i - j$ sites are unoccupied. Therefore each cluster is characterized by two integer numbers and thus a cluster (i, j) consists of i connected particles and j linkers in state 1 or j occupied sites (see Fig. 1(a)). Two clusters will aggregate when one unoccupied site in one cluster bonds to an occupied site in the other.

There are then two distinct aggregation mechanisms:

1) *Free linkers bond to clusters* (i, j) (see Fig. 1(c)). When a free linker and a cluster (i, j) meet, the free linker bonds to an unoccupied site of the cluster with probability $p_0(i, j)$ that equals the fraction of unoccupied sites of the cluster,

$$p_0(i, j) = \frac{w_i - j}{w_i}. \quad (2)$$

If the bonding succeeds a cluster $(i, j+1)$ is formed.

2) *Cluster-cluster aggregation*. When a cluster (i_1, j_1) and a cluster (i_2, j_2) meet, they can aggregate if a bond is formed between an unoccupied and an occupied site of each cluster (see Fig. 1(d)). They will do so with probability $p(i_1, j_1; i_2, j_2)$ that equals the product of the fraction of unoccupied and occupied sites of each cluster,

$$p(i_1, j_1; i_2, j_2) = \frac{j_1(w_{i_2} - j_2) + j_2(w_{i_1} - j_1)}{w_{i_1}w_{i_2}}. \quad (3)$$

This aggregation results in a cluster $(i_1 + i_2, j_1 + j_2 - 1)$.

The restrictions to aggregation expressed by Eqs. (2) and (3) incorporate in the dynamics the limited number of linkers that a particle can support in a simple way. In both cases, each aggregation event is considered to be instantaneous: the formation of a bond is much

faster than all other processes and may be considered instantaneous compared to the other relevant time scales (diffusion limited aggregation). In addition, since we focus on the limit of low density of particles and linkers (see below), the timescale of the linker-mediated aggregation is sufficiently large for the shape and orientation of each cluster to be uncorrelated between successive bonding events. As a consequence (as already expressed in (2) and (3)), every site of the “surface” of a cluster is equally likely to form the next bond.

The relevant time scales are set by the translational diffusion coefficients of the particles, D_P , and the free linkers, D_L (see Fig. 1(b)). For simplicity, all clusters have the same diffusion coefficient (i.e. D_P). We define as control parameter the ratio Δ of the diffusion coefficients,

$$\Delta = \frac{D_L}{D_P}. \quad (4)$$

We consider the limit where the linkers diffuse faster than the particles (i.e. $\Delta \geq 1$), since it is reasonable to assume that the linkers have a lower mass (and size) than the particles.

Finally, since we consider the low density limit, it is assumed that a free linker and a cluster (of any size) occupy the same volume, thus setting a single and trivial length scale. Notice that, within this approximation, the density is simply an initial condition for the dynamics, as the aggregation process will effectively decrease it.

In summary, this model for linker-particle aggregation has three relevant parameters: f , the particle valence; ϕ , the ratio between the number of linkers and the maximum number of available sites for the linkers to bond, and Δ , the ratio of the diffusion coefficients of linkers and particles. Numerical simulations and an approximate Smoluchowski equation are used to investigate the aggregation dynamics for several values of ϕ and Δ .

B. Numerical Simulations

N_P particles (or clusters $(1, 0)$) and $N_L = \phi f N_P$ free linkers are randomly distributed without overlap on a simple cubic lattice with N_{latt} sites and periodic boundary conditions, each occupying one lattice site. The initial density of particles $\rho \equiv N_P/N_{\text{latt}}$ is set to a low value ($\rho = 0.1$ for the simulations reported) and f is chosen to be 6. The diffusive motion of the clusters and free linkers is described by kinetic Monte Carlo simulations. At each iteration, one cluster or one free linker is chosen and attempt a hop to a randomly chosen neighbouring lattice site. Free linkers are chosen with probability $\kappa_L N_0/Q$ and clusters of size i with probability $\kappa_P m_i/Q$, where N_0 and m_i are the actual numbers of free linkers and of clusters of size i , respectively, Q is the total hopping rate,

$$Q = \kappa_L N_0 + \kappa_P \sum_i m_i, \quad (5)$$

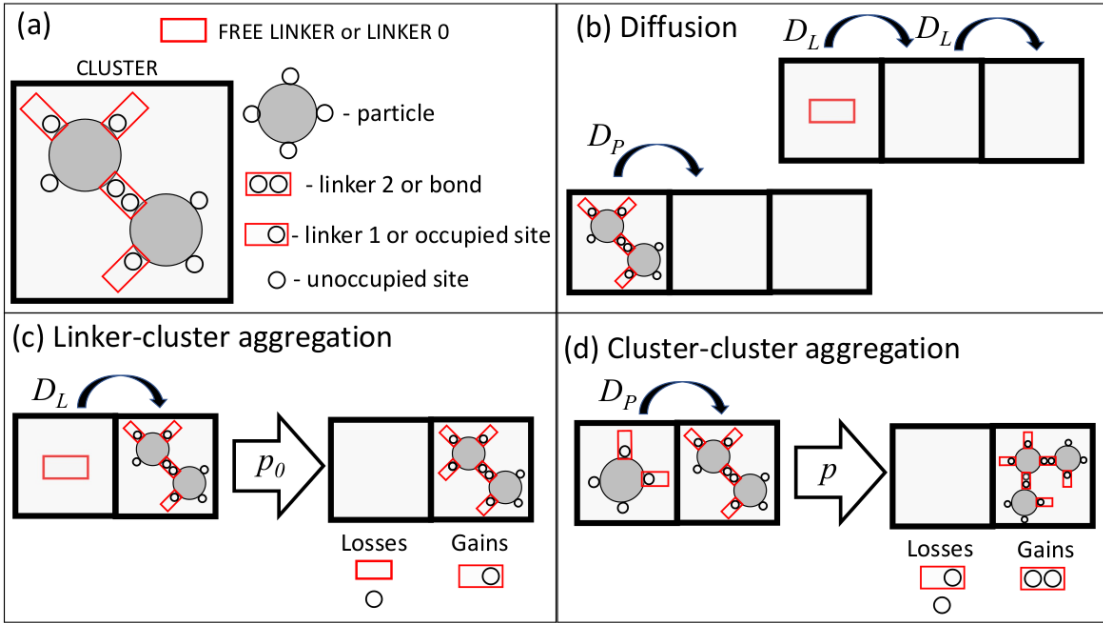


Figure 1. Schematic representation of the model. (a) The constituents of the system are free linkers (or linkers in state 0) and clusters. A cluster (i, j) consists of i particles (each can be bonded to a maximum of f other particles) and has j sites occupied (out of $w_i = (f - 2)i + 2$), and $w_i - j$ sites unoccupied; since the cluster is tree like, it has $i - 1$ bonds. An occupied site is a linker in state 1 and a bond is a linker in state 2. In the example of the figure $f = 4$, $i = 2$ and $j = 3$; therefore $w_i = 6$, there is 1 bond (or linker 2) and 3 unoccupied sites. (b) Diffusion. The constituents diffuse randomly: linkers with a diffusion coefficient D_L and clusters (of all sizes) with a diffusion coefficient D_P . Only cases where $D_L \geq D_P$ are considered. (c) Linker-cluster aggregation happens with probability p_0 (given by Eq. (2)) when a free linker encounters a cluster (i, j) . After bonding to the cluster, the free linker turns into a linker 1 while the cluster gains an occupied and loses an unoccupied site. The same bonding happens with equal probability when a cluster encounters a free linker. (d) Cluster-cluster aggregation happens with probability p (given by Eq. (3)) when two clusters meet. The size of the new cluster is the sum of the sizes of the clusters that merged; as a consequence one occupied and one unoccupied sites (one in each cluster) disappear and a new bond forms. In the example of the figure, clusters (1, 2) and (2, 3) aggregate to form a cluster (3, 4).

and κ_L, κ_P are two hopping rates that can be related to the diffusion coefficients of the linkers and particles (see below). For a linker, depending on the state (occupied or empty) of the randomly chosen neighbouring site, the hop is:

- (i) Accepted if it is not occupied;
- (ii) Rejected if it is occupied by another free linker;
- (iii) Rejected/accepted with probability $1 - p_0(i, j) / p_0(i, j)$ (given by Eq. (2)) when it is occupied by a cluster (i, j) ; when accepted the cluster (i, j) is updated to a cluster $(i, j + 1)$, and the free linker is changed to a linker of type 1 contained in the new cluster.

Similarly, for a cluster (i_1, j_1) , depending on the state of the randomly chosen neighbouring site, the hop is:

- (i) Accepted if it is not occupied;
- (ii) Rejected/accepted with probability $1 - p_0(i, j) / p_0(i, j)$ (given by Eq. (2)) if it is occupied by a free linker; when accepted the cluster (i, j) is updated to a cluster $(i, j + 1)$ and the free linker is changed to a linker of type 1 contained in the new cluster;

- (iii) Rejected/accepted with probability $1 - p(i_1, j_1; i_2, j_2) / p(i_1, j_1; i_2, j_2)$ (given by Eq. (3)) if it is occupied by a cluster (i_2, j_2) ; when accepted the clusters (i_1, j_1) and (i_2, j_2) disappear by merging into a cluster $(i_1 + i_2, j_1 + j_2 - 1)$.

Notice that, since each cluster and each free linker occupies one lattice site, the number of occupied lattice sites decreases by one whenever a free linker bonds to a particle site or a linker-mediated bond is formed.

The discrete hopping process is transformed into continuous diffusion by: (i) using the relations [26] $\kappa_L = 6D_L/a^2$ and $\kappa_P = 6D_P/a^2$, where a is the lattice constant; (ii) incrementing time, at each iteration, by a random number that follows a Poisson distribution with average value $1/Q$. The values of N_0 , m_i and Q are updated as a result of the aggregation that follows from the encounter of the diffusive linkers and clusters.

Simulations were performed on a lattice of size $N_{\text{latt}} = 25^3$, with $N_P = \rho N_{\text{latt}} = 1562$ particles; 10^3 samples were run for each pair (Δ, ϕ) . For $\Delta = 10$ and some values of ϕ , runs were performed also on lattices of sizes $N_{\text{latt}} = 16^3$ and 32^3 at the same density ρ , to check for finite size effects that turned out to be negligible.

C. Smoluchowski equations

The aggregation dynamics implemented in the simulations is described by the generalized Smoluchowski equation described in what follows.

Let m_{ij} be the number of clusters (i, j) . Then, the rate at which m_{ij} changes is,

$$\dot{m}_{ij} = K_{0,+} - K_{0,-} + K_+ - K_-, \quad (6)$$

where:

1. $K_{0,+}$ is the rate at which free linkers bond to clusters $(i, j-1)$ and form a (i, j) cluster,

$$K_{0,+} = (\kappa_P + \kappa_L) p_0(i, j-1) \frac{N_0 m_{i(j-1)}}{N_{\text{latt}}}; \quad (7)$$

2. $K_{0,-}$ is the rate at which free linkers bond to (i, j) clusters,

$$K_{0,-} = (\kappa_P + \kappa_L) p_0(i, j) \frac{N_0 m_{ij}}{2N_{\text{latt}}}; \quad (8)$$

3. K_+ is the rate at which two clusters bond to form a (i, j) cluster,

$$K_+ = \kappa_P \sum_{i_1+i_2=i} \sum_{j_1+j_2=j+1} p(i_1, j_1; i_2, j_2) \frac{m_{i_1 j_1} m_{i_2 j_2}}{N_{\text{latt}}}; \quad (9)$$

4. K_- is the rate at which a cluster (i, j) bonds to other clusters,

$$K_- = 2\kappa_P \sum_{i_1=1}^{\infty} \sum_{j_1=0}^{w_{i_1}} p(i_1, j_1; i, j) \frac{m_{i_1 j_1} m_{ij}}{N_{\text{latt}}}. \quad (10)$$

The description of the dynamics of aggregation is completed with the equation for the time evolution of the free linkers, i.e. the rate at which free linkers bond to clusters (thus changing their state from 0 to 1),

$$\dot{N}_0 = - \sum_{i=1}^{\infty} \sum_{j=0}^{w_i} K_{0,-} = (\kappa_P + \kappa_L) N_0 \sum_{i=1}^{\infty} \sum_{j=0}^{w_i} p_0(i, j) \frac{m_{ij}}{N_{\text{latt}}}. \quad (11)$$

The aggregation dynamics for clusters of size i can be obtained from Eq. (6) by using $m_i = \sum_{j=0}^{w_i} m_{ij}$ and taking into account that $\sum_{j=0}^{w_i} (K_{0,+} - K_{0,-}) = 0$,

$$\begin{aligned} \dot{m}_i = & \frac{\kappa_P}{N_{\text{latt}}} \sum_{j_1=1}^{w_{i_1}} \sum_{j_2=1}^{w_{i_2}} p(i_1, j_1; i_2, j_2) m_{i_1 j_1} m_{i_2 j_2} - \\ & - \frac{2\kappa_P}{N_{\text{latt}}} \sum_{i_1=1}^{\infty} \sum_{j=1}^{w_i} \sum_{j_1=0}^{w_{i_1}} p(i, j; i_1, j_1) m_{i_1 j_1} m_{ij}. \end{aligned} \quad (12)$$

This equation shows that (3) defines the kernel of the aggregation process. It is well known that the form of the

kernel determines the time evolution of the cluster size distribution, and that analytical solutions can only be obtained in a few particular cases [26]. Since there is no analytical solution for the kernel (3), approximations are required. Nevertheless, its resemblance to known analytically solvable cases suggests the expected behaviour of the solution. The numerator of (3) is similar to a polymerization kernel, since it can increase faster than linearly with the cluster sizes, thus accelerating the aggregation process; however, the denominator “normalizes” the kernel by the product of the cluster sizes, rendering it similar to a constant kernel. Therefore, one can anticipate similarities of the dynamics to the constant kernel aggregation, namely the absence of critical percolation (i.e. the impossibility of forming a giant cluster in finite time).

D. Scaling hypothesis for the cluster size distribution

In this section we show that it is possible to approximate the full Smoluchowski description of eq. (12) by an analytically solvable equation, if a scaling hypothesis for m_{ij} is adopted. As demonstrated below, this scaling hypothesis is equivalent to assuming that, at any given instant, the fraction j/w_i of occupied sites of a cluster (i, j) is independent of the size i of the cluster and equals the ratio between the total number of unoccupied sites (or linkers 1) and the total number of sites of the clusters. Inspired by the fact that the kernel $p(i_1, j_1; i_2, j_2)$ in Eq. (3) is a function of j_1/w_{i_1} and j_2/w_{i_2} , we assume the following *Ansatz* for the cluster size distribution m_{ij} ,

$$m_{ij}(t) = m_i(t) \frac{g(j/w_i, t)}{\sum_{j=0}^{w_i} g(j/w_i, t)}, \quad (13)$$

where $g(x, t)$ is a time dependent scaling function. Furthermore, the moments of this function are calculated by replacing the sum by an integral,

$$\sum_{j=0}^{w_i} j^k g(j/w_i, t) = w_i^{k+1} \int_0^1 x^k g(x, t) dx. \quad (14)$$

A simple approximation for the time evolution of the cluster size distribution $m_i(t)$ is then obtained by using (13) and (14) in (12),

$$\dot{m}_i(t) = \frac{2\kappa_P}{N_{\text{latt}}} q(1-q) \left(\sum_{i_1+i_2=i} m_{i_1} m_{i_2} - 2m_i \sum_{i_1=0}^{\infty} m_{i_1} \right), \quad (15)$$

where,

$$q = \frac{\int_0^1 x g(x, t) dx}{\int_0^1 g(x, t) dx}. \quad (16)$$

Likewise, the time evolution of the free linkers is obtained by substituting (13) and (14) in (11),

$$\dot{N}_0 = -\frac{\kappa_L + \kappa_P}{N_{\text{latt}}} N_0 (1 - q) \sum_{i=1}^{\infty} m_i. \quad (17)$$

Notice that the quantity q has a simple physical meaning: the number of linkers in state 1 is $N_1 \equiv \sum_{ij} j m_{ij}$, which may be written as,

$$N_1 = q \sum_{i=1}^{\infty} w_i m_i, \quad (18)$$

i.e., q is the ratio of the actual number of linkers in state 1 and its maximum value for a cluster size distribution m_i . Moreover, if (13) and (14) are used to replace the numerator in (16), we obtain,

$$q = \frac{\sum_{j=0}^{w_i} j m_{ij}}{w_i m_i} \equiv \frac{N_{1,i}}{w_i m_i}, \quad (19)$$

which means that within the approximation the fraction of the linkers 1 bonded to clusters of size i at a given instant is independent of i . It is also possible to determine the time evolution of N_2 using (15) (and recalling that the clusters are tree like),

$$\dot{N}_2 \equiv - \sum_{i,j} \dot{m}_{ij} = \frac{2\kappa_P}{N_{\text{latt}}} q (1 - q) (N_P - N_2)^2. \quad (20)$$

The time evolution of the number of free linkers N_0 can be expressed as (performing the sums in (17)),

$$\dot{N}_0 = -\frac{\kappa_L + \kappa_P}{N_{\text{latt}}} (1 - q) N_0 (N_P - N_2). \quad (21)$$

The time evolution of the fraction of linkers in state i , $p_i \equiv N_i/N_L$, is then given by,

$$\begin{cases} \dot{p}_0 = -\frac{1+\Delta}{2} p_0 (1 - q) (1 - f\phi p_2) \end{cases} \quad (22)$$

$$\begin{cases} \dot{p}_2 = \frac{q(1-q)(1-f\phi p_2)^2}{f\phi} \end{cases} \quad (23)$$

$$\begin{cases} q = \phi \frac{1-p_0-p_2}{1-2\phi p_2}, \end{cases} \quad (24)$$

where $\Delta = \frac{\kappa_L}{\kappa_P} = \frac{D_L}{D_P}$ is the ratio (4) between the two time scales and the time has been rescaled by $t \rightarrow 2\rho\kappa_P t$. These equations will be solved numerically for fixed values of Δ and ϕ and initial conditions $p_0(0) = 1$ and $p_2(0) = 0$ (i.e. all linkers are free and all clusters are $(1, 0)$ at $t = 0$, as in the simulations). Notice that the time evolution for the fraction of linkers in state 1 can be obtained from $p_1 = 1 - p_0 - p_2$. Similarly, the ratio between the actual number of bonds between particles, N_2 , and the maximum number of those bonds, $fN_P/2$ (that we designate by bonding probability, p_b), is also obtained as a function of time, as $p_b = 2\phi p_2$.

Finally, this approximation yields an expression for the cluster size distribution m_i as a function of p_2 . Dividing (15) by (20) gives,

$$\frac{(1 - f\phi p_2)^2}{f\phi} N_P \frac{dm_i}{dp_2} = \sum_{i_1=1}^{i-1} m_{i_1} m_{i-i_1} - 2m_i \sum_{i_1=1}^{\infty} m_{i_1}, \quad (25)$$

which, after a change of variables to $z = 1/(1 - f\phi p_2) - 1$, becomes,

$$N_P \frac{dm_i}{dz} = \sum_{i_1=1}^{i-1} m_{i_1} m_{i-i_1} - 2c_i \sum_{i_1=1}^{\infty} m_{i_1}. \quad (26)$$

This equation is formally equivalent to that obtained for the time evolution of clusters with a constant kernel [26], and its solution (for the initial condition $m_i(z=0) = N_P \delta_{i,1}$) is,

$$m_i = N_P \frac{z^{i-1}}{(1+z)^{i+1}}. \quad (27)$$

Using the relation between z and p_2 , the cluster size distribution m_i can be expressed as a function of p_2 ,

$$m_i = N_P (1 - f\phi p_2)^2 (f\phi p_2)^{i-1}. \quad (28)$$

Since $z = 0$ is equivalent to the initial condition used in the simulations ($p_2 = 0, p_0 = 1$), then (28) is the theoretical prediction for the time evolution of the cluster size distribution. Notice that, as in the aggregation with constant or polymerization kernels, the cluster size distribution depends on time through the bonding probability only. The total number of clusters is $M_0 \equiv \sum_{i=1}^{\infty} m_i = N_P (1 - f\phi p_2)$ and the second moment of the cluster size distribution is $M_2 \equiv \sum_{i=1}^{\infty} i^2 m_i = N_P \frac{1+f\phi p_2}{1-f\phi p_2}$.

III. RESULTS

The dynamics of the model is obtained through simulations at several values of (Δ, ϕ) for $f = 6$ using the same initial conditions (free linkers at $t = 0$: $p_0(0) = 1, p_2(0) = 0$). The results are compared with theoretical calculations based on the approximations discussed in the previous section. This comparison tests the validity of those approximations. In the following we present and discuss the asymptotic regimes of the dynamics, the time evolution of the bonding probabilities, and the time evolution of the cluster size distribution.

A. Asymptotics

The asymptotic states of the model may be found by considering the aggregation rules and the nature of the clusters. A tree like cluster with i particles has, by definition, $i - 1$ linker-mediated bonds. Thus, for the

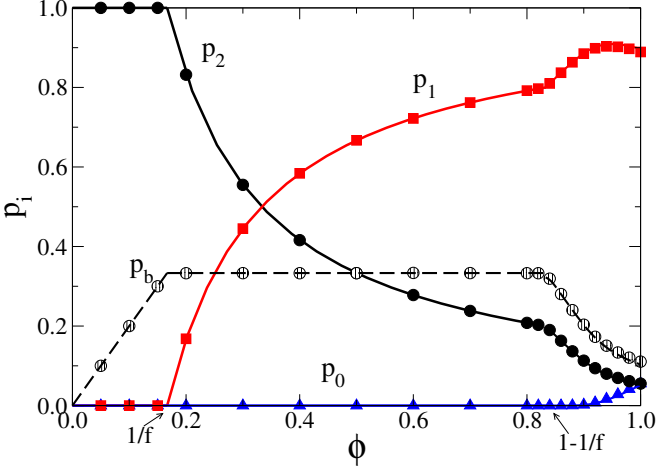


Figure 2. Asymptotic values of the probabilities p_i as a function of ϕ for $f = 6$ and $\Delta = 10$. The symbols represent simulation results and the lines the theoretical results from Eqs. (22,23). Three different regimes are observed for $\phi < 1/f$, $1/f < \phi < 1 - 1/f$ and $\phi > 1 - 1/f$. Only the latter is Δ dependent (see Fig. 3).

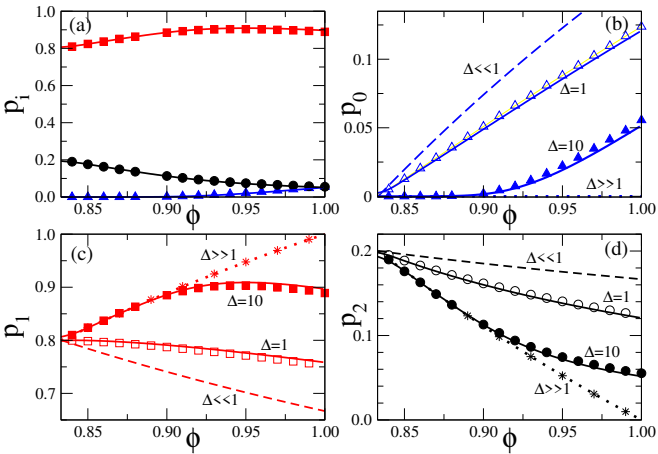


Figure 3. Asymptotic values of the probabilities p_i for different values of Δ in the regime $\phi > 1 - 1/f$ (numerical results for $f = 6$). The symbols represent simulation results and the lines the theoretical results from Eqs. (22,23). (a) $\Delta = 10$ (a blow up of part of Fig. 2); (b), (c) and (d) depict p_0 , p_1 and p_2 respectively. The different symbols and lines correspond to different values of Δ as indicated. The analytical expressions when $\Delta \gg 1$ and $\Delta \ll 1$ may be found in the text. The asterisks in (c) and (d) are simulation results for $\Delta = 100$.

model under study, the actual number of linker-mediated bonds, N_2 , must obey $N_2 < N_P$ (or $p_2 < 1/(f\phi)$). Moreover, since each particle can bond to at most f linkers the number of occupied sites is $N_1 \leq fN_P$ (or $p_1 \leq 1/\phi$). In Fig. 2 we plot the asymptotic values of the bonding probabilities p_i and the bonding fraction $p_b \equiv N_2/(fN_P/2) = 2\phi p_2$, as a function of ϕ for $\Delta = 10$. We find three different asymptotic regimes depending on the values of ϕ :

1) $0 < \phi < \frac{1}{f}$. In this regime the total number of linkers is less than the total number of particles. In fact, the number of linkers is so low that all the linkers will establish bonds between the particles (i.e. all linkers 0 become linkers 2). The time taken to form these bonds depends on Δ (as discussed below) but not the final state: $p_2 = 1$ and $p_1 = p_0 = 0$, which is a fixed point of Eqs. (22) and (23). Due to the tree like character of the clusters, $N_2 < N_P$ or $p_2 \leq 1/(f\phi)$, and this regime will occur when $\phi < 1/f$. The asymptotic value of the bonding probability p_b grows linearly with ϕ up to its maximum value $2/f$. These results are independent of Δ (for simplicity only $\Delta = 10$ is shown in Fig. 2).

2) $\frac{1}{f} < \phi < 1 - \frac{1}{f}$. In this regime, the number of linkers is larger than the total number of particles but smaller than $N_P(f-1)$. The number of bonds between the particles takes its maximum value $p_2 = 1/(f\phi)$ and the bonding probability, $p_b = 2/f$, is maximal and independent of ϕ . Since $N_L > N_P$ or $\phi > 1/f$, the number of type 1 linkers is non-zero $N_1 = N_L - N_P$ or $p_1 = 1 - 1/(f\phi)$ (and $p_0 = 0$). This regime corresponds to the fixed point $p_0 = 0$, $p_2 = 1/(f\phi)$ of Eqs. (22) and (23), and will occur when $\phi < 1 - 1/f$, since $p_1 + p_2 = 1 \leq 1/(f\phi) + 1/\phi$. The asymptotic state is also independent of Δ , and is shown in Fig. 2 for $\Delta = 10$. The same results are obtained for any other value of Δ . The constant bonding fraction $p_b = 2/f$ implies that in this regime there is a single cluster, which contains all the particles, in the limit $t \rightarrow \infty$.

3) $\phi > 1 - \frac{1}{f}$. In this regime the asymptotic state is determined by the exhaustion of unoccupied sites in the clusters. At $t = 0$, the number of unoccupied sites is fN_P ; since each linker 1 occupies one site and each linker 2 occupies two sites, the fraction of unoccupied sites at any time is $1 - \phi(p_1 + 2p_2)$, and vanishes when $p_1 + 2p_2 = 1/\phi$. The values of p_1 and p_2 which satisfy this condition depend on Δ . This can be seen by analysing two limiting cases. When $\Delta \gg 1$, the N_L linkers, free at $t = 0$, change to linkers 1 before any bonds between the clusters are formed; at this stage there are N_L linkers 1 and $fN_P - N_L$ unoccupied sites that will then start to form bonds between the particles or clusters; at the end of this process, there are $fN_P - N_L$ bonds ($p_2 = 1/\phi - 1$) and $2N_L - fN_P$ linkers 1 ($p_1 = 2 - 1/\phi$), and the aggregation stops since all the sites are occupied. In the other limit, when $\Delta \ll 1$, when a free linker bonds to an unoccupied site a bond between two clusters is also formed between the newly occupied site and an unoccupied one; this process lasts while N_2 remains below its maximum value N_P ($p_2 = 1/(f\phi)$). Thereafter the remaining free linkers $N_L - N_P$ will bond with the $(f-2)N_P$ still unoccupied sites; this second process ends when $N_1 = (f-2)N_P$ (or $p_1 = (1 - 2/f)/\phi$), as all the sites are occupied. Notice that at this stage a number of linkers are still free as $N_0 = N_L - (f-1)N_P$ (or $p_0 = 1 - (1 - 1/f)/\phi$) is non-zero. The asymptotic state for finite values of Δ lies between these limits. This regime corresponds to the fixed point $q = 1$ of Eqs. (22) and (23). In Figs. 2

and 3(a) we show the asymptotic values of p_i for $\Delta = 10$ and $1 - 1/f < \phi < 1$, obtained from the simulations and the theory, which are in quantitative agreement. Figures 3(b)-(d) illustrate this for other values of Δ and reveal the same excellent agreement between the simulation and the theoretical results.

We conclude that the asymptotic numbers of bonds and clusters depend on the ratio of the diffusion coefficients Δ only when $N_L > (f - 1)N_P$. Faster free linkers (larger Δ) promote the depletion of unoccupied sites decreasing the formation of bonds between the clusters. For intermediate values of N_L , i.e. $1/f < \phi < 1 - 1/f$, the model predicts the formation of a single cluster, containing all the particles, in the long time limit.

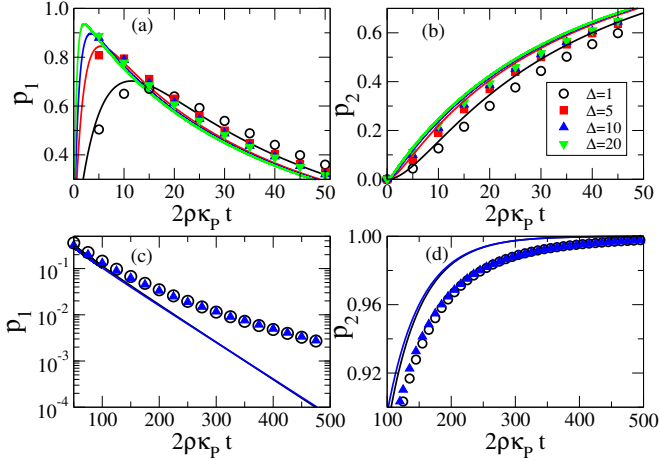


Figure 4. Time evolution of the probabilities p_1 ((a) and (c)) and p_2 ((b) and (d)) at fixed $\phi = 0.05$ and the indicated values of Δ , at short ((a) and (b)) and long ((c) and (d)) times. The symbols represent simulation results and the lines are numerical solutions of Eqs. (22), (23). For the sake of clarity, in (c) and (d) only the results for $\Delta = 1$ and $\Delta = 10$ are shown (the results are independent of Δ).

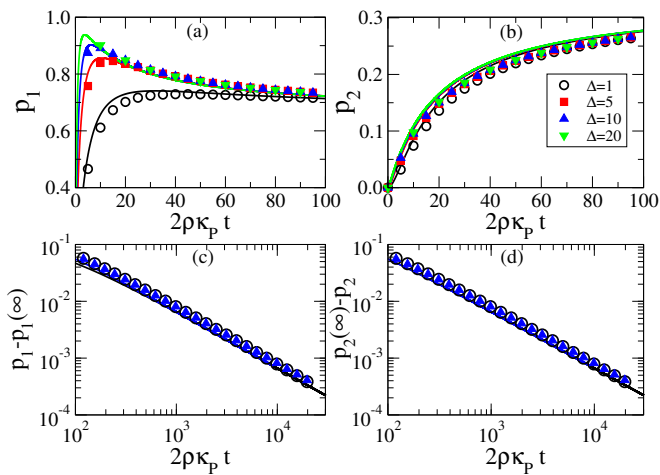


Figure 5. Time evolution of p_1 and p_2 as in Fig. 4 at $\phi = 0.5$.

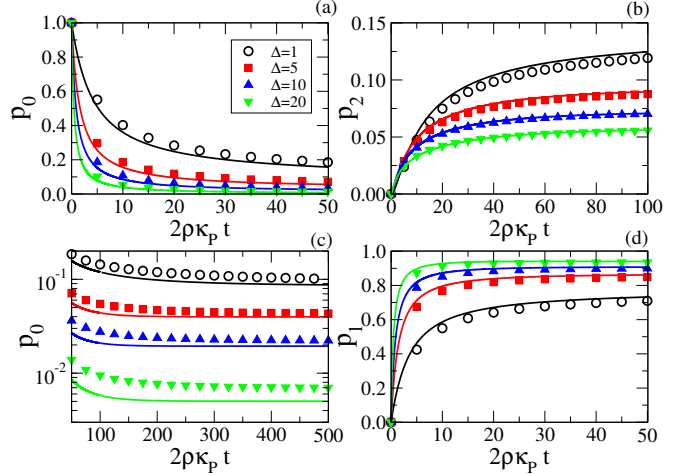


Figure 6. Time evolution of p_0 , p_1 and p_2 as in Figs. 4 and 5 at $\phi = 0.95$.

B. Time evolution of the bonding probabilities

We consider the dynamics of the aggregation at three different values of $\phi = 0.05$, 0.5 and 0.95 (representative of the three asymptotic regimes), and different diffusion ratios, $\Delta = 1, 5, 10$ and 20 . We keep $f = 6$ fixed. At the two lowest values of ϕ , the fraction of linkers of type 1, p_1 , exhibits a maximum at early times. The value of this maximum increases and the time when it occurs decreases as Δ increases (see Figs. 4(a) and 5(a)). The presence of the maximum signals the change from an initial regime dominated by the formation of bonds between free linkers and unoccupied sites to a second regime where bonds between the particles form and the clusters merge. This transition is absent at $\phi = 0.95$ (see Fig. 6 (d)): if the fraction of free linkers is sufficiently high bond formation between free linkers and unoccupied sites dominates at all times, due to the large decrease of unoccupied sites required for the formation of bonds between clusters. Figs. 4 and 5 show that, at low ϕ , the time evolution of the bonding probabilities can be divided into an initial Δ dependent regime (up to $2\rho\kappa_P t \approx 50 - 100$, Figs. 4 and 5 (a), (b)) and a late Δ independent regime (Figs. 4 and 5 (c), (d)). By contrast, at large values of ϕ the dynamics depends on Δ at all times (see Fig. 6).

The theoretical results are validated by comparing them to the results of simulations (lines and symbols in Figs 4-6). At low $\phi = 0.05$, initially, there is qualitative agreement for the time evolution of p_1 and p_2 , including their dependence on Δ (Fig. 4(a) and (b)). At late times, there is agreement on the prediction that the dynamics does not depend on Δ (Figs. 4(c) and (d)). However, a quantitative discrepancy has been observed: while the theory predicts fast exponential decay to the asymptotic values, the simulation reveals a slower time evolution. At $\phi = 0.5$ (Fig. 5) the agreement between the theory and simulations is almost quantitative at all values of Δ .

Both predict a power-law decay of the evolution of the probabilities at late times, with an exponent ≈ -1 (Figs. 5(c) and (d)). This feature results from the non-linearity of Eq. (23), which for $1/f < \phi < 1 - 1/f$, and $t \rightarrow \infty$ reduces to,

$$\dot{x} = -B(f, \phi)x^2, \quad (29)$$

where $x = 1 - f\phi p_2$ and $B(f, \phi) = (f - 1 - f\phi)(f\phi - 1)/(f - 2)^2$. The solution of this equation yields $p_1(t) - p_1(t = \infty) = 1/(Bf\phi t)$. This power law decay was observed in simulations for other values of ϕ in the range $1/f < \phi < 1 - 1/f$, which strongly suggests that the present model in this range behaves as irreversible aggregation with a constant kernel [26].

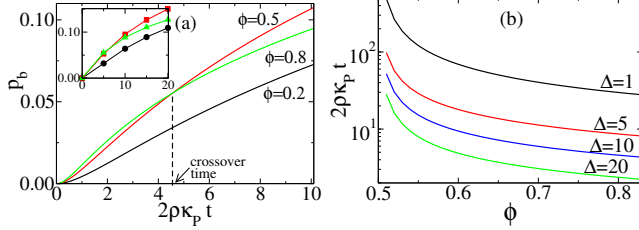


Figure 7. (a) Bonding probability, p_b , as a function of time at the early stages for $\Delta = 10$ and for three values of ϕ . The lines represent theoretical results Eqs. (22,23). The crossover time, where p_b at $\phi = 0.5$ equals p_b at $\phi = 0.8$, is indicated. The inset displays the simulation results for the same parameters, namely, $\phi = 0.2$ (circles), $\phi = 0.5$ (squares) and $\phi = 0.8$ (triangles); in the inset the lines are guides to the eye. (b) Crossover time as a function of ϕ for different values of Δ .

The maximum number of bonds between particles (mediated by type 2 linkers) is reached asymptotically whenever $1/f < \phi < 1 - 1/f$ for any Δ as discussed in section III A (see Fig. 2). In this regime, the system tends to form a single cluster that contains all particles. In order to investigate the conditions (ϕ, Δ) under which the time required for the aggregation of this cluster is minimal, we analyse Eqs. (22,23) in the limits $t \rightarrow 0^+$ and $t \rightarrow \infty$, to obtain the behaviour of the bonding fraction p_b in these limits. At $t = 0$, one has $\dot{p}_b = 0$ and $\ddot{p}_b = \phi(1 + \Delta)/f$, and therefore,

$$\lim_{t \rightarrow 0^+} p_b(t) = \phi \frac{1 + \Delta}{f} t^2. \quad (30)$$

As a consequence, the initial growth of the clusters increases with Δ and ϕ . The limit $t \rightarrow \infty$ may be obtained using Eq. (29) as $p_b = 2/f(1 - x)$ and thus,

$$\lim_{t \rightarrow \infty} p_b(t) = \frac{2}{f} \left(1 - \frac{1}{B(f, \phi)t} \right). \quad (31)$$

The function $B(f, \phi)$ has a maximum at $\phi = 0.5$. Thus, for any f and Δ , the single cluster limit will be approached faster when $\phi = 0.5$. This behaviour is illustrated in Fig. 7(a), where the value of p_b for $f = 6$ and

$\Delta = 10$ is plotted for $\phi = 0.2, 0.5$ and 0.8 , as obtained from the theory and simulations. Initially, the fastest growth is obtained for the largest ϕ ($\phi = 0.8$). However, the bonding fractions for $\phi = 0.8$ and $\phi = 0.5$ cross at $t \approx 5$ (in the units used in the figure) and the bonding fraction for $\phi = 0.5$ becomes the largest at later times. Figure 7(b) represents this crossover time as a function of $\phi \in [0.5; 1 - 1/f]$ for several values of Δ . This result may have experimental relevance: if the goal is the growth of the largest cluster in the shortest time then, for a given number of N_P particles, the optimal number of linkers is $N_L = fN_P/2$, irrespecte of their difusion coefficients.

C. Cluster size distributions

The total number of clusters is the zeroth moment, M_0 , of the cluster size distribution m_i . It is, by definition, related to the number of linkers in state 2, $M_0 = N_P - N_2$, since the clusters are tree like. As a consequence, the mean cluster size, $\langle S_1 \rangle \equiv N_P/M_0$, can be calculated from p_2 : $\langle S_1 \rangle = 1/(1 - f\phi p_2)$. In Figs. 8 (a) and (c), $\langle S_1 \rangle^{-1}$ is represented for $\Delta = 10$, $f = 6$. $\langle S_1 \rangle$ grows with time, but the extent of this growth depends on ϕ . At $\phi < 1/f$ it reaches the asymptotic value $\langle S \rangle = 1/(1 - f\phi)$ – see fig. 8(a). At $\phi > 1 - 1/f$, the asymptotic value of $\langle S_1 \rangle$ depends on Δ . In both cases, the growth of large clusters is strongly limited as we observed $\langle S_1 \rangle < 2$ at all times. By contrast, when $1/f < \phi < 1 - 1/f$, there is no finite asymptotic limit for $\langle S_1 \rangle$, as shown in Fig. 8(c). The mean cluster size grows monotonically with time; the dependence on ϕ is limited to the time taken to reach a given cluster size, which has a minimum at $\phi = 0.5$ (at times larger than the crossover described in Fig. 7). The results in Fig. 8(a) at $\phi = 0.05$ and 0.95 reveal that the agreement between simulations and theory is good while those in Fig. 8(c) at $\phi = 0.5$ and 0.2 show that the theory slightly overestimates $\langle S_1 \rangle$ at long times.

The cluster size distribution was determined using simulations for $\Delta = 10$, $f = 6$ at several values of ϕ and different times. The inverse of M_2 , the second moment of these distributions, divided by N_P , is represented in Figs. 8(b) and (d), as a function of $(1 - fp_b/2)/(1 + fp_b/2)$ to facilitate the comparison with the theoretical prediction. A behaviour similar to that of $\langle S_1 \rangle$ is observed: limited growth at $\phi = 0.05$ and 0.95 and an asymptotic divergence at $\phi = 0.2$ and 0.5 . The theory overestimates M_2 in all cases except at $\phi = 0.5$.

The fraction of clusters of a given size i , m_i/M_0 , is represented in Fig. 9 at several values of ϕ and three different times, corresponding to $p_b \approx 0.5p_b(\infty)$, $p_b \approx 0.75p_b(\infty)$ and $p_b \approx p_b(\infty)$. The theoretical results are obtained using Eq. (28) for the fraction of clusters of size i ,

$$\frac{m_i}{M_0} = \left(1 - \frac{fp_b}{2} \right) \left(\frac{fp_b}{2} \right)^{i-1}, \quad (32)$$

where $p_b = 2\phi p_2$. At the initial stage of growth, the clus-

ter size distributions are exponential for every ϕ and the agreement between Eq. (32) and the results of simulation is excellent. As time progresses, we find that this distribution is still exponential for large i , at $\phi = 0.05$ and $\phi = 0.95$ (see Figs. 9(a) and (b)), but the agreement between theory and simulations is poor. The theory predicts an exponential distribution for all sizes and largely underestimates the frequency of large clusters. These differences are compatible with the results reported in Figs. 8(a) and (b): theory and simulation agree for the number of small clusters and for $\langle S_1 \rangle$ (which is dominated by the contribution of the more abundant small clusters); on the other hand, as large clusters have a more significant contribution to M_2 , the broader distributions observed in the simulations yield a larger M_2 than that predicted by the theory.

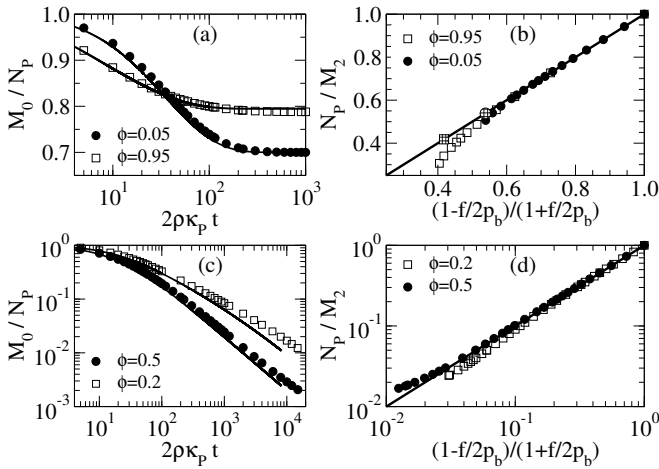


Figure 8. Inverse mean cluster size, M_0/N_P ((a) and (c)) as a function of time, and inverse second moment of the cluster size distribution ((b) and (d)), N_P/M_2 , as a function of $(1 - fp_b/2)/(1 + fp_b/2)$. $\Delta = 10$ and $f = 6$ in all cases; the values of ϕ are indicated in the figures. The symbols are the results from simulations and the lines from Eqs. (22), (23) and (32). The patterned symbols in (b) indicate the asymptotic values predicted by the theory at $\phi = 0.95$ (square) and $\phi = 0.5$ (circle).

There is a remarkable agreement between the cluster size distributions obtained by simulations and theory at $\phi = 0.5$ (see Fig. 9(c)). At this value of ϕ the asymptotic value of p_b is $2/f$, and thus the distribution Eq. (32) becomes a very slow varying function of i for values of p_b close to $2/f$. Both theory and simulation exhibit a very broad cluster size distribution (almost uniform in the simulations) at the highest value of p_b in Fig. 9(c). To test if this agreement is obtained at other values of $\phi \in [1/f; 1 - 1/f]$, the results at $\phi = 0.2$ are shown in Fig. 9(d). Exponential distributions are obtained at low and intermediate values of p_b and for large cluster sizes only when p_b is close to $2/f$. The theory underestimates both the number of very small and very large clusters. Still, the broadness of M_0 is reached asymptotically in both theory and simulations.

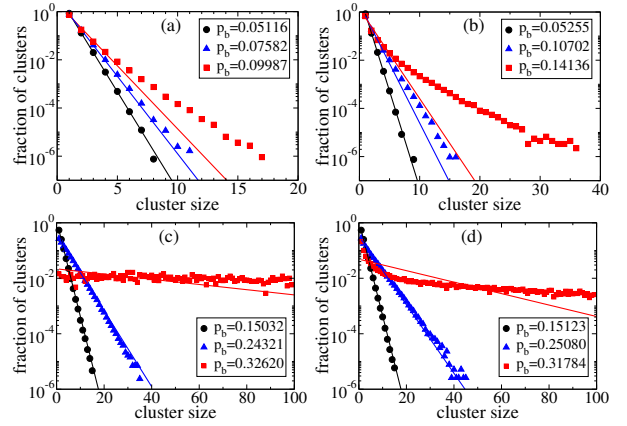


Figure 9. Fraction of the clusters of a given size for $\Delta = 10$, $f = 6$ at different times (corresponding to the values of p_b). (a) $\phi = 0.05$; (b) $\phi = 0.95$; (c) $\phi = 0.5$, (d) $\phi = 0.2$. Symbols are the simulation results and the lines are obtained from Eq. (32) at the indicated values of p_b . In all cases, lines with larger (absolute) slopes correspond to larger values of p_b .

IV. CONCLUSIONS AND DISCUSSION

We have studied a simple model of linker-mediated irreversible aggregation of particles with a maximum valence f . This process was analysed using simulations and a simplified version of the Smoluchowski equations. Simulations have shown that the dynamics and the cluster size distributions are determined by ϕ (the ratio between the actual number of linkers and the maximum number of linkers to which particles can bond or total number of bonding sites) and by Δ (the ratio between the diffusion coefficients of linkers and clusters) in a non-trivial way. In particular, ϕ alone determines the asymptotic state of the system when $\phi < 1 - 1/f$, while for $\phi > 1 - 1/f$ (i.e. for a large number of linkers) the asymptotic state will depend also on Δ . The cluster size distributions obtained at both low ($< 1/f$) and high ($> 1 - 1/f$) ϕ are exponential and exhibit finite and small moments at all times. On the other hand, for $\phi \in [1/f; 1 - 1/f]$ the distribution becomes very broad asymptotically, with a diverging second moment. In this interval, the initial growth of the clusters is faster at larger values of ϕ and Δ ; however, after a crossover time that depends on Δ , the system with $\phi = 0.5$ exhibits always the fastest growth and the largest clusters (at a given time).

The results of the approximate Smoluchowski equations (15,17) are in line qualitatively (and in some cases quantitatively) with the simulation results. This comparison tests the validity of the assumption that the fraction of unoccupied sites of a cluster is independent of its size. This hypothesis works quantitatively at the initial stages of growth but fails drastically at low ($< 1/f$) and high ($> 1 - 1/f$) ϕ by failing to capture correctly the cluster size distributions at large times. This means that, at least at low and high ϕ , there is a relevant non-trivial

time evolution of the dependence on the cluster size of the fraction of unoccupied sites that is not captured by the theory. The theory makes the strong prediction that the cluster size distribution (32) depends on time only through the bonding probability p_b , and the comparison with the simulations shows that this is valid for values of $\phi \in [1/f; 1 - 1/f]$. Any extension of this theory would have to include a ϕ and size dependence on the fraction of occupied sites of a cluster. The cluster size distribution (32) of the linker-mediated aggregation is equal to that obtained for a constant kernel [26], and therefore the model proposed in this work, with dynamics determined by a “normalized” polymerization kernel (3), turns out to be similar to the model of irreversible aggregation with a constant kernel. In particular, the absence of percolation (i.e. the formation of a giant cluster in a finite time) and the asymptotic broad distribution at large times reinforce the similarity with the linker-mediated aggregation model in the range $\phi \in [1/f; 1 - 1/f]$.

The goals to investigate a linker-mediated aggregation model were the study of the effects of limited linker-particle aggregation and the existence of two diffusion time scales. One could extend this study further by adding other more realistic ingredients to the model: geometrical (and not just “topological”) clusters, size dependent diffusion coefficients, clusters with loops, etc. In accordance, the theory would have to be improved to include, amongst other new ingredients, correlations in the distribution of the unoccupied sites.

V. ACKNOWLEDGMENTS

We acknowledge financial support from the Portuguese Foundation for Science and Technology (FCT) under Contracts no. PTDC/FIS-MAC/28146/2017 (LISBOA-01-0145-FEDER-028146), UIDB/00618/2020, UIDP/00618/2020, and CEECIND/00586/2017.

[1] K. Ariga, M. Nishikawa, T. Mori, J. Takeya, L. K. Shrestha, and J. P. Hill, *Science and Technology of Advanced Materials* **20**, 51 (2019).

[2] V. N. Manoharan, *Science* **349**, 1253751 (2015).

[3] A. van Blaaderen, M. Dijkstra, R. van Roij, A. Imhof, M. Kamp, B. W. Kwaadgras, T. Vissers, and B. Liu, *Euro. Phys. J. Special Topics* **222**, 2895 (2013).

[4] V. Privman, in *Complex-Shaped Metal Nanoparticles: Bottom-Up Syntheses and Applications* (2012) pp. 239–268.

[5] L. Cademartiri, K. J. M. Bishop, P. W. Snyder, and G. A. Ozin, *Phil. Trans. R. Soc.* **370**, 2824 (2012).

[6] B. Ruzicka, E. Zaccarelli, L. Zulian, R. Angelini, M. Sztucki, A. Moussaïd, T. Narayanan, and F. Sciortino, *Nature Mater.* **10**, 56 (2010).

[7] J. Dobnikar, A. Snezhko, and A. Yethiraj, *Soft Matt.* **9**, 3693 (2013).

[8] S. L. Elliott, R. J. Butera, L. H. Hanus, and N. J. Wagner, *Faraday discuss.* **123**, 369 (2003).

[9] N. Geerts and E. Eiser, *Soft Matt.* **6**, 4647 (2010).

[10] D. Nykypanchuk, M. M. Maye, D. van der Lelie, and O. Gang, *Nature* **451**, 549 (2008).

[11] C. S. Dias, N. A. M. Araújo, and M. M. Telo da Gama, *Adv. Col. Interf. Sci.* **247**, 258 (2017).

[12] D. Joshi, D. Bargteil, A. Caciagli, J. Burelbach, Z. Xing, A. S. Nunes, D. E. P. Pinto, N. A. M. Araújo, J. Bruijc, and E. Eiser, *Sci. Adv.* **2**, e1600881 (2016).

[13] G. C. Antunes, C. S. Dias, M. M. da Gama, and N. A. M. Araújo, *Soft Matter* **15**, 3712 (2019).

[14] A. Singh, B. A. Lindquist, G. K. Ong, R. B. Jadrish, A. Singh, H. Ha, C. J. Ellison, T. M. Truskett, and D. J. Milliron, *Angew. Chem. Int. Ed.* **54**, 14840 (2015).

[15] B. Bharti, J. Meissner, S. H. L. Klapp, and G. H. Findenegg, *Soft Matter* **10**, 718 (2014).

[16] J. Peng, A. Kroes-Nijboer, P. Venema, and E. van der Linden, *Soft Matt.* **12**, 3514 (2016).

[17] K. W. Müller, R. F. Bruinsma, O. Lieleg, A. R. Bausch, W. A. Wall, and A. J. Levine, *Physical Review Letters* **112**, 238102 (2014).

[18] C. J. Cyron, K. W. Müller, K. M. Schmoller, A. R. Bausch, W. A. Wall, and R. F. Bruinsma, *EPL* **102**, 38003 (2013).

[19] B. A. Lindquist, R. B. Jadrish, D. J. Milliron, and T. M. Truskett, *J. Chem. Phys.* **145**, 074906 (2016).

[20] J. Lowensohn, B. Oyarzún, G. Narváez Paliza, B. M. Mognetti, and W. B. Rogers, *Phys. Rev. X* **9**, 41054 (2019).

[21] N. Ghofraniha, P. Andreozzi, J. Russo, C. La Mesa, and F. Sciortino, *The journal of physical chemistry. B* **113**, 6775 (2009).

[22] N. Brilliantov, P. L. Krapivsky, A. Bodrova, F. Spahn, H. Hayakawa, V. Stadnichuk, and J. Schmidt, *Proceedings of the National Academy of Sciences* **112**, 9536 (2015).

[23] H. Hayakawa and S. Hayakawa, *Astronomical Society of Japan* **40** (1988).

[24] E. Hicks, M. R. Wiesner, and C. K. Gunsch, *Water Research* **171**, 115438 (2020).

[25] K. Harton and S. Shimizu, *Biophysical Chemistry* **247**, 34 (2019).

[26] P. L. Krapivsky, S. Redner, and E. Ben-Naim, *A Kinetic View of Statistical Physics* (Cambridge University Press, New York, 2011) pp. 1–488.